

Organometallic Ruthenium Nanoparticles as a Model of Study for Fischer-Tropsch Synthesis Reaction

L. M. Martinez-Prieto*, K. Philippot* and B. Chaudret**

* CNRS, LCC (Laboratoire de Chimie de Coordination), 205 Route de Narbonne, BP44099, F-31077 Toulouse Cedex 4, France ; Université de Toulouse, UPS, INPT, F-31077 Toulouse Cedex 4, France, luis-miguel.martinez@lcc-toulouse.fr, karine.philippot@lcc-toulouse.fr

** LPCNO; Laboratoire de Physique et Chimie des Nano-Objets, UMR5215 INSA-CNRS-UPS, Institut des Sciences appliquées, 135, Avenue de Rangueil, F-31077 Toulouse, France, chaudret@insa-toulouse.fr

ABSTRACT

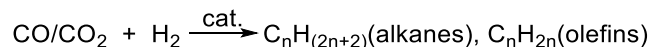
Three samples of organometallic ruthenium nanoparticles (RuNPs) namely Ru-PVP (PVP=polyvinylpyrrolidone; 1.3 nm), Ru-dppb (dppb=diphenylphosphinobutane; 1.9 nm) and Ru-heptanol-dppb (3.1 nm) were prepared and investigated in a model Fischer-Tropsch Synthesis (FTS) reaction. Our aim was to shed some light on the influence of the metal core size and of the chemical environment at the metal surface on the surface reactivity of these RuNPs through the hydrogenation of CO into hydrocarbons (olefins and paraffins). For that purpose, we used a combination of spectroscopic techniques such as gas phase and solid state NMR, MS and FTIR. The results evidence that the size increase of the metal core does not affect significantly the catalytic properties of the RuNPs since comparable conversion and selectivity are obtained with Ru-dppb and Ru-heptanol-dppb. In the contrary, the stabilizer seems to have a crucial role in directing the catalytic reaction.

Keywords: ruthenium nanoparticles, surface chemistry, fischer tropsch synthesis (FTS), size and stabilizer effect

1 INTRODUCTION

Promising solution to the limited stock of natural sources of hydrocarbons and to control the CO and CO₂ emissions is the controlled Fischer-Tropsch Synthesis (FTS), where CO and CO₂ are hydrogenated to produce hydrocarbons (olefins and paraffins) (Scheme 1) [1]. The development of more active and/or selective catalysts for FTS is still a challenging field of research [2]. Indeed, the activity and selectivity of FTS have been improved over several decades but fundamental issues about the mechanism and the structure of the catalyst remain unsolved. Although iron and cobalt containing catalysts have been preferred by the industry for economic reasons, ruthenium is known as the most active metal for CO

hydrogenation. Ruthenium is able to produce high molecular weight hydrocarbons at low temperature (~150 °C) and pressure (<100 bar) [3]. Thus, Ru nanoparticles (RuNPs) can provide more efficient and selective catalytic performance, and they are considered as a system of choice to investigate surface chemistry studies during a model FTS reaction [4-11].



Scheme 1: Fischer Tropsch Synthesis: Alkanes and olefins production through the hydrogenation of CO and CO₂.

In our team, we have a strong experience in the synthesis of well-defined metal nanoparticles (NPs) following an organometallic approach [12]. This method of synthesis allows the fine tuning of NP size and surface chemistry through addition of appropriate ligands as stabilizers. Such systems of nanoparticles are thus of interest to apprehend precisely the influence of the metal core size and of the surface ligand on the catalytic performance of NPs in model FTS. With this objective we prepared a set of organometallic RuNPs of different size and/or chemical surface environment - Ru-PVP (PVP=polyvinylpyrrolidone; 1.3 nm), Ru-dppb (dppb=diphenylphosphinobutane; 1.9 nm) and Ru-heptanol-dppb (3.1 nm) and studied their surface reactivity in the hydrogenation of CO under simulated reaction conditions. Nuclear Magnetic Resonance (NMR) and Fourier-Transformation Infrared (FTIR) spectroscopies were used to probe the surface chemistry of the RuNPs.

PVP and dppb stabilized RuNPs (with a mean size of 1.3 for Ru-PVP and 1.9 nm for Ru-dppb nm, respectively) were first synthesized and involved in a FTS model catalytic reaction to study the influence of the stabilizer on the surface chemistry of the particles. Second, the behavior of larger RuNPs (3 nm, Ru-heptanol-dppb) while keeping a similar ligand shell (dppb) was also studied. The synthesis

and characterization of these Ru-heptanol-dppb NPs is reported here for first time.

This work evidences that the size of the ruthenium core does not affect the activity and selectivity of the RuNPs in the chosen model FTS reaction. The major effect through this study came from the surface modification when the dppb ligand is coordinated.

2 RESULTS

2.1 Ru NPs Synthesis and Characterization

The synthesis of the Ru NPs is based on the decomposition of Ru(COD)(COT) under 3 bar H₂ in mild conditions and in the presence of a stabilizer whose role is to control the characteristics of the nanoparticles in terms of size and surface chemical environment. The RuNPs were prepared using a polymer (PVP, polyvinylpyrrolidone) or ligands namely 1,4-bis(diphenylphosphino)butane (dppb) or a mixture of heptanol/dppb. PVP is added in a large excess and stabilizes the nanoparticle through a steric mode. In contrast, dppb is a σ -donor and a weak π -acceptor bidentate ligand that is known to strongly coordinate to the metal surface. These samples were respectively named Ru-PVP and Ru-dppb and were synthesized according to a previously reported procedure [13]. In order to evaluate the size effect, we also developed a new synthetic route to obtain larger RuNPs with a similar surface state, namely Ru-heptanol-dppb. These novel Ru-heptanol-dppb NPs were synthesized by a two-step procedure: first, weakly stabilized Ru-heptanol NPs were prepared by decomposition of [Ru(cod)(cot)] under 3 bar H₂ in heptanol [14], and second a ligand exchange was achieved, where the heptanol was displaced by the strong electron donor dppb ligand (Figure 1). In all the cases the NPs obtained are crystalline, monodisperse and very-well distributed.

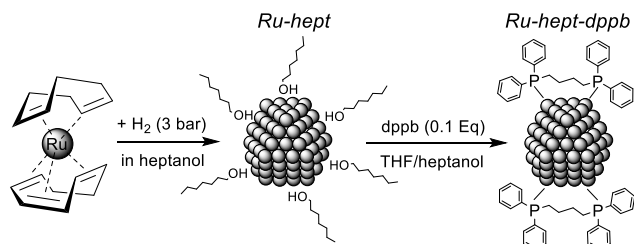


Figure 1: Two-step route followed for the synthesis of Ru-hept-dppb NPs

With these three RuNP samples (Figure 2) we had in hand a system of choice to evaluate first the influence of dppb ligand on the surface chemistry of small RuNPs in a FTS model reaction by comparing the reactivity of Ru-PVP (1.3 nm) and Ru-dppb (1.9 nm). Furthermore, we could study the size effect of the metal core on CO hydrogenation by comparing the activity and selectivity of dppb-stabilized

Ru NPs of 1.9 nm (Ru-dppb) and 3.1 nm (Ru-heptanol-dppb) whose surface chemical environment is similar.

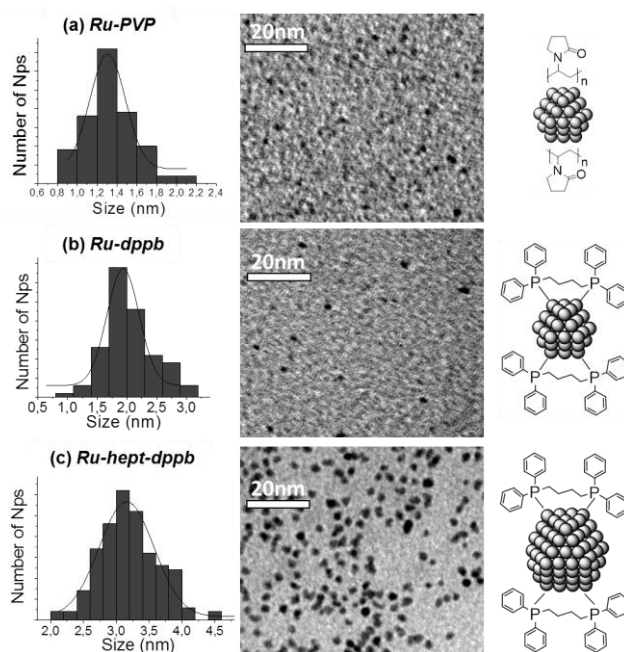


Figure 2: Schematic structure, TEM images and corresponding size-distributions for Ru-PVP (a) Ru-dppb (b) and Ru-hept-dppb (c) NPs.

Wide-Angle X-ray Scattering (WAXS) of Ru-heptanol-dppb reveals that NPs are well crystallized according to hexagonal closed packed (hcp) structure. Although the RDF doesn't indicate oxidation, it shows a complex situation: the Ru-Ru distances are not so well-defined and the shape of the envelope is not consistent with a single size system. First distances are consistent with hcp structure and a coherence length of 2.7 nm. If we compare with a theoretical model corresponding to particles of similar coherence length, we can see the discrepancy (Figure 3). Ru-heptanol-dppb sample probably contains a large majority of small domains of ca. 1.5 nm in size, and a minority of much larger domains of ca. 2.7 nm, strongly distorted compared to a perfect hcp pattern.

High Resolution Transmission Electron Microscopy (HRTEM) images (Figure 4) show the presence of both irregularly shaped polycrystalline and mono-crystalline particles. No considerable structural difference can be observed between Ru-heptanol and Ru-heptanol-dppb samples. Fourier analysis applied to HRTEM images confirms that the Ru NPs retain the hcp structure of bulk Ru. For example, the Fourier transform in figure 1 (a) corresponds to a $\langle 2-1-10 \rangle$ zone axis of bulk Ru and the four labeled spots can be indexed as follows: spot 1 (0002), spot 2 (01-11), spot 3 (01-10), spot 4 (01-1-1). Moreover, HRTEM analysis on different specimens shows that the largest particles are polycrystalline and that the size of the

average mono-crystalline domains is compatible with the coherence length determined by WAXS. As expected, Ru-heptanol-dppb NPs exhibit a similar size (3.1 nm) as its precursor Ru-hept NPs (3 nm) but have the ligand dppb coordinated on their surface.

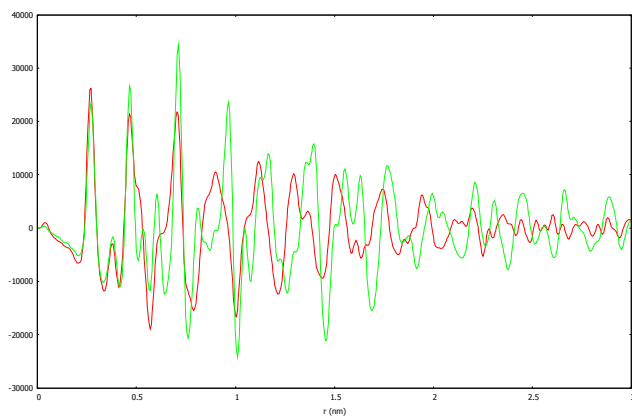


Figure 3: WAXS analysis of *Ru-hept-dppb* NPs (red) and comparison with theoretical data for RuNPs of similar coherence length (green).

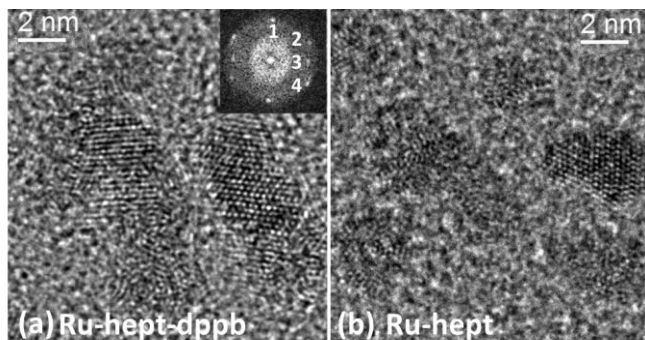


Figure 4: HRTEM images of *Ru-hept-dppb* (a) and *Ru-hept* (b) NPs. The inset in (a) shows the Fourier transform of one *Ru-hept-dppb* NP.

The coordination of the dppb ligand on the surface of *Ru-heptanol-dppb* NPs was evidenced by solid state NMR and Fourier-Transformation Infrared (FTIR). $^{31}\text{P}\{^1\text{H}\}$ Magic Angle Spinning (MAS) NMR spectrum showed a peak around 35 ppm, corresponding to the coordinated diphenylphosphine. The presence of dppb was also evidenced by $^{13}\text{C}\{^1\text{H}\}$ MAS-NMR: expected peaks at 129 ppm (aromatic carbons) and at 25 ppm (the alkyl chain) are observed as well as signals that can be attributed to heptanol remaining on the metal surface (Figure 5a). Coordination of CO and characterization by IR and solid state NMR spectroscopies have been also used to understand the surface chemistry of the particles and the location of the active sites. When *Ru-hept-dppb* NPs were pressurized with 0.6 bar of ^{13}CO (r.t. during 20 h), two peaks corresponding to CO groups adsorbed on the metal surface were detected: a broad peak at $\delta \sim 230$ ppm assigned to ^{13}CO coordinated in a bridging mode (CO_b), probably situated on

the faces, and a sharp peak at $\delta = 196$ ppm corresponding to ^{13}CO coordinated in a terminal mode (CO_t). The presence of spinning bands suggests that the CO_t are static (Figure 5b). On CP MAS NMR spectrum, the intensity of the signal for bridging COs is decreased compared that corresponding to terminal ones. This can be attributed to the location of the latter in the vicinity of hydrogen carriers (dppb). These results are in agreement with the existence of diverse surface sites on the particles.

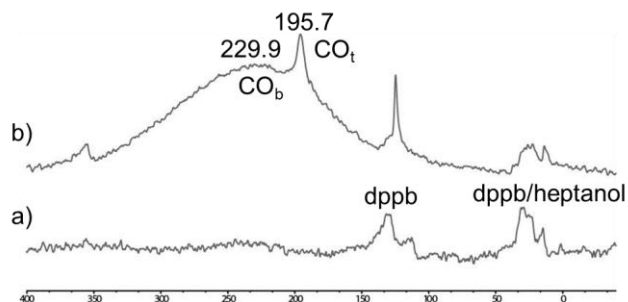


Figure 5: a) Solid-state ^{13}C MAS-NMR spectrum of *Ru-hept-dppb* NPs. b) Solid-state $^{13}\text{C}\{^1\text{H}\}$ MAS-NMR spectrum of *Ru-hept-dppb* NPs after reaction with ^{13}CO (0.6 bar; 20h; r.t.)

Surprisingly, before any exposure to CO, the characteristic frequency of coordinated CO on Ru surface (ca. 1939 cm^{-1}) was already visible (Figure 7), which means that CO groups are formed during the synthesis of the particles. This can be explained by a partial decarbonylation of heptanol in the reaction conditions of synthesis. Such reaction is known in the literature where several examples of decarbonylation of alcohols catalyzed by Ru complexes are available [14-16].

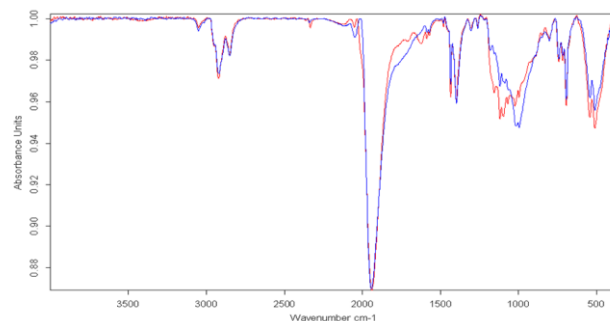


Figure 6: IR spectra registered for *Ru-hept-dppb* NPs before (blue) and after (red) adsorption of CO (0.6 bar, r.t., 20 h).

2.2 Preliminary Reactivity Studies

The activity and selectivity of the *Ru-PVP*, *Ru-dppb* and *Ru-hept-dppb* NPs for FTS was quantified using gas phase NMR and Mass spectrometry (MS). The reactions were carried out in 2 ml quick pressure valve NMR tubes. These NMR tubes were filled with NPs as powders (0.02-0.05 mmol of Ru^0) and then pressurized with 3 bar of syngas

(1:1 molar mixture of H₂ and ¹³CO) before heating at 120-150 °C for 1-5 days. Preliminary results revealed that Ru-PVP NPs are not active at 120 °C. Meanwhile Ru-dppb and Ru-heptanol-dppb NPs have a similar activity at 120 °C, consuming around 20-30% of the H₂. The poor activity of Ru-PVP was confirmed at 150 °C, consuming only the 8 % of the total dihydrogen. Otherwise Ru-dppb and Ru-heptanol-dppb consumed all the dihydrogen under these conditions. From these preliminary data it appears that a size increase does not affect appreciably the activity of the NPs, but the presence of the dppb ligand improves it strongly. Regarding the selectivity, it is important to highlight that all Ru nanocatalysts here described produced mostly methane and light hydrocarbons (alkanes and olefins). In particular Ru-dppb and Ru-heptanol-dppb showed a higher selectivity than Ru-PVP for C₂-C₄ hydrocarbons vs methane: at 150 °C the first ones formed ca. 85 % of C₂-C₄ alkanes/alkenes and Ru-PVP only ca. 45 %. This result is of interest regarding the selectivity in FTS, considering that Ru is often reported as producing essentially of methane.

3 CONCLUSIONS

A new synthesis of ruthenium nanoparticles (Ru-heptanol-dppb (3 nm)) was developed and together with Ru-PVP (1.3 nm) and Ru-dppb (1.9 nm) form a range of nanocatalysts displaying a diversity of sizes. By this way we could study the influence of the metal core size while keeping the same ligand shell provided by the coordination of the dppb ligand. From the results obtained in the FTS reaction used as model of study, it appears that the size increase of the ruthenium core does not affect significantly the catalytic properties of the NPs. The major effect observed came from the surface modification by dppb, as the coordination of dppb at the metal surface leads to highly active FTS Ru nanocatalysts with interesting selectivities for C₂-C₄ alkanes and alkenes under mild reaction conditions (120-150 °C; 3 bar of syngas).

Thus, the design of novel hybrid organic-inorganic Ru nanoparticles may provide new catalysts for FTS reaction, where NPs catalytic properties are tuned through the inorganic core and the ligand shell.

4 ACKNOWLEDGEMENTS

The authors thank CNRS, University Paul Sabatier at Toulouse University, Institut des Sciences Appliquées at Toulouse (INSA) as well as V. Collière, P. F. Fazzini and L. Datas for TEM facilities (TEMSCAN, UPS) and P. Lecante (CEMES, CNRS) for WAXS measurements and C. Bijani and Y. Coppel for gas phase and solid state NMR measurements. This work was supported by EU (ERC Advanced Grant - NANOSONWINGS 2009-246763).

REFERENCES

- [1] Schulz, H. Short History and Present Trends of Fisher-Tropsch Synthesis. *Appl. Catal. A: Gen.* 186, 3, 1999.
- [2] M. E. Dry, A. P. Steynberg, in *Fischer-Tropsch Technol.* (Ed.: A.S. and M.D.B.T.-S. in S.S. and Catalysis), Elsevier, 406, 2004.
- [3] Vannice, M. A. *Catal. Rev.* 1976, 14, 153.
- [4] K. Xiong, J. Li, K. Liew, X. Zhan, *Appl. Catal. A Gen.* 389, 173, 2010.
- [5] X.-Y. Quek, Y. Guan, R. a. van Santen, E. J. M. Hensen, *ChemCatChem*, 3, 1735, 2011.
- [6] J. M. González Carballo, E. Finocchio, S. García, S. Rojas, M. Ojeda, G. Busca, J. L. G. Fierro, *Catal. Sci. Technol.* 1, 1013, 2011.
- [7] A.-X. Yin, W.-C. Liu, J. Ke, W. Zhu, J. Gu, Y.-W. Zhang, C.-H. Yan, *J. Am. Chem. Soc.* 134, 20479, 2012.
- [8] C. Wang, H. Zhao, H. Wang, L. Liu, C. Xiao, D. Ma, *Catal. Today* 183, 143, 2012.
- [9] P. Lignier, R. Bellabarba, R. P. Tooze, Z. Su, P. Landon, H. Ménard, W. Zhou, *Cryst. Growth Des.* 12, 939, 2012.
- [10] J. M. G. Carballo, E. Finocchio, S. García-Rodríguez, M. Ojeda, J. L. G. Fierro, G. Busca, S. Rojas, *Catal. Today* 214, 2, 2013.
- [11] J. Kang, S. Zhang, Q. Zhang, Y. Wang, *Angew. Chem. Int. Ed. Engl.* 48, 2565, 2009.
- [12] Organometallic derived-I: Metals, Colloids and Nanoparticles, Philippot K. and Chaudret B., in *Comprehensive Organometallic Chemistry III*, Carberry R. H. & Mingos M. P. (Eds.: In chief), Elsevier, Vol 12; Patricia, L.; Philippot, K.; Chaudret, B. *ChemCatChem* 5, 28, 2013.
- [13] J. García-Antón, M. R. Axet, S. Jansat, K. Philippot, B. Chaudret, T. Pery, G. Buntkowsky, H.-H. Limbach, *Angew. Chem. Int. Ed. Engl.* 47, 2074, 2008.
- [14] Y. Z. Chen, W. C. Chan, C. P. Lau, H. S. Chu, H. L. Lee *Organometallics*, 16, 1241, 1997.
- [15] b) P. D. Bolton, M. Grellier, N. Vautravers, L. Vendier, S. Sabo-Etienne *Organometallics*, 27, 5088, 2008.
- [16] L. S. Van der Sluys, G. J. Kubas, K. G. Caulton *Organometallics*, 10, 1033, 1991.
- [17] C. Pan, K. Pelzer, K. Philippot, B. Chaudret, F. Dassenoy, P. Lecante, M. J. Casanove, *J. Am. Chem. Soc.* 123, 7584, 2001.
- [18] K. Pelzer, K. Philippot, B. Chaudret, *Zeitschrift für Phys. Chemie* 2003, 217, 1539.